JGP Journal of General Physiology

RESEARCH ARTICLE

On the role of transient depolarization-activated K^+ current in microvillar photoreceptors

Roman V. Frolov

Photoreceptors in the compound eyes of most insect species express two functional types of depolarization-activated potassium currents: a transient A-type current (IA) and a sustained delayed rectifier current (IDR). The role of Shaker-dependent IA in *Drosophila melanogaster* photoreceptors was previously investigated by comparing intracellular recordings from *Shaker* and wild-type photoreceptors. Shaker channels were proposed to be involved in low-frequency signal amplification in dim light and reduction of the metabolic cost of information transfer. Here, I study the function of IA in photoreceptors of the cockroach *Panchlora nivea* using the patch-clamp method. Responses to Gaussian white-noise stimuli reveal that blockade of IA with 4-aminopyridine has no discernible effect on voltage responses or information processing. However, because open-channel blockers are often ineffective at low membrane potentials, no conclusion on the role of IA could be made on the basis of negative results of pharmacological tests. Using a relatively large set of control data, a physiological variability analysis was performed to discern the role of IA. Amplitudes of the IA window current and half-activation potentials correlate strongly with membrane corner frequencies, especially in dim light, indicating that IA facilitates transmission of higher frequencies. Consistent with voltage-dependent inactivation of IA, these correlations decrease with depolarization in brighter backgrounds. In contrast, correlations involving IDR are comparatively weak. Upon reexamining photoreceptor conductance in wild-type and *Shaker* strains of *D. melanogaster*, I find a biphasic voltage dependence near the resting potential in a minority of photoreceptors from both strains, indicating that Shaker channels are not crucial for early amplification of voltage signals in *D. melanogaster* photoreceptors. Leak current in *Shaker* photoreceptors at the level of the soma is not elevated. These results suggest a novel role for IA in facilitating transmission of high-frequency signals in microvillar photoreceptors.

Introduction

Photoreceptors in the majority of insect species express two functional types of voltage-activated potassium currents (Kv) that counter membrane depolarization and modulate graded voltage responses to light stimulation: a transient A-type (IA) and one or more sustained delayed rectifier (IDR) currents (Laughlin and Weckström, 1993; Weckström and Laughlin, 1995; Frolov et al., 2016). IA is a rapidly activating current that inactivates fully within less than a second at voltages corresponding to responses in moderately bright light. In *Drosophila melanogaster*, IA is mediated by Shaker channels (Hardie et al., 1991). Early patch-clamp recordings revealed that these two conductances had very different voltage dependencies, with the half-activation potential (HAP) of IA more than 20 mV more negative than that of IDR (Hevers and Hardie, 1995).

The role of IA in *D. melanogaster* photoreceptors was investigated by comparing electrophysiological phenotypes of *Shaker* null mutants (Sh^{KS133}) and wild-type flies in intracellular recording experiments (Juusola et al., 2003; Niven et al., 2003a,b). In addition to the deletion of IA, several changes were found in the mutant photoreceptors, including a large leak conductance, strongly reduced signal and noise variances with low voltage gain, high membrane corner frequencies, a uniformly low signal-to-noise ratio, and low information rates.

It was proposed that IA is responsible for low-frequency amplification of voltage responses in dim light through the following mechanism. At rest, IA conductance is partly activated, whereas IDR channels are closed and do not start opening until the membrane is substantially depolarized, usually by tens of millivolts. Because inactivation of IA at rest is insignificant, IA forms a persistent current. However, as the membrane is depolarized by light-activated channels, inactivation of IA increases drastically. Because persistent IA is observed in a relatively

Faculty of Science, Nano and Molecular Materials Research Unit, University of Oulu, Oulu, Finland.

Correspondence to Roman V. Frolov: rvfrolov@gmail.com.

https://doi.org/10.1085/jgp.201711940

narrow voltage range between the resting potential and several millivolts above it, this constitutes a "window" current. As IA inactivates progressively with membrane depolarization, the total membrane conductance might decrease depending on the activation threshold for Shab channels, and amplify low-frequency voltage signals (Niven et al., 2003b). It was also argued that as the metabolic cost of photoreceptor signaling in *Shaker* null mutants is higher than in wild-type flies, expression of Shaker channels reduces it accordingly (Niven et al., 2003a).

The role of IA was examined in several other species, including crane flies and locusts (Weckström and Laughlin, 1995; Laughlin, 1996). In locust photoreceptors, the total Kv current undergoes striking circadian changes from a sustained current during the day to a strongly inactivating, IA-like current during the night (Cuttle et al., 1995). This arrangement is thought to be instrumental in reducing the metabolic cost of photoreceptor functioning (Weckström and Laughlin, 1995). In the crane fly, photoreceptor properties evolved for optimal operation in the dark, with only one rapidly inactivating repolarizing Kv conductance found. Its function was suggested to suppress high-frequency noise (Laughlin, 1996). In the cockroach *Periplaneta americana*, patch-clamp recordings found a relatively small IA, of unknown molecular basis, and a large IDR, which is mostly based on ether-a-go-go channels (Salmela et al., 2012; Immonen et al., 2017). Computer modeling indicated that voltage responses to contrast-modulated light in the absence of IA would be no different from control and would not be altered even if IA was increased ten-fold (Salmela et al., 2012).

In the present work, I investigated the role of IA in photoreceptor functioning using whole-cell patch-clamp recordings combined with acute pharmacological blockade of IA in photoreceptors of *Panchlora nivea*, a flying cockroach species characterized by a prominent IA and a small delayed rectifier (Frolov et al., 2017). Although, in contrast to *D. melanogaster*, voltage activation ranges for IA and IDR coincide in *P. nivea*, IA is characterized by a prominent window current between −60 and −40 mV (Frolov et al., 2017), which can be expected to modulate voltage responses in relatively dim light stimulation backgrounds. I show that the IA appears to be responsible for expansion of signaling bandwidth under low and intermediate illumination conditions.

In addition, because the conclusions of the *D. melanogaster* Shaker studies cited above were primarily based on data obtained from intracellular recordings, I reexamined the underlying assumptions of the early nonlinear amplification hypothesis (Juusola et al., 2003; Niven et al., 2003b) by comparing photoreceptor conductances in wild-type and Sh^{KS133} mutant flies using prolonged patch-clamp recordings. I found that although the dependence of total membrane conductance on membrane potential in some photoreceptors was indeed consistent with the previous observations and could provide some signal amplification, such photoreceptors were in the minority. Importantly, similar observations were also made in Sh^{KS133} mutants, implying that this phenomenon is not based solely on Shaker channels. In addition, I show that at the level of photoreceptor soma, leak conductance is not increased in Sh^{KS133} in comparison to control flies.

Materials and methods

Animals

Cuban cockroaches (*P. nivea*) of both sexes were purchased from Virginia Cheeseman, Entomological Supplier. *D. melanogaster* wild-type Canton Special (CS), mutant Sh^{KS133}, and wild-type *Drosophila virilis* strains were maintained in the laboratory.

Patch-clamp recordings

Animal preparation and whole-cell patch-clamp recordings from *P. nivea* photoreceptors were performed as described previously (Frolov et al., 2017). In brief, data were acquired using an Axopatch 1-D patch-clamp amplifier with pClamp software (Axon Instruments/Molecular Devices). Electrodes were made from borosilicate glass (World Precision Instruments) and had resistance of 4–8 MΩ. Bath solution contained (in mM) 120 NaCl, 5 KCl, 4 $MgCl_2$, 1.5 $CaCl_2$, 10 *N*-Tris-(hydroxymethyl)-methyl-2-amino-ethanesulfoncic acid (TES), 25 proline, and 5 alanine, pH 7.15. Patch pipette solution contained (in mM) 120 K-glutamate plus 20 KCl, 10 TES, 2 $MgCl_2$, 4 Mg-ATP, 0.4 Guanosine 5′-triphosphate sodium salt hydrate (Na-GTP), and 1 NAD, pH 7.15. All chemicals were purchased from Sigma-Aldrich. The liquid junction potential (LJP) between bath and intracellular solution was −12 mV. Only green-sensitive photoreceptors were used in experiments. A light-emitting diode with a peak wavelength at 525 nm combined with a series of neutral density filters (0 to 8 log units of attenuation) was used for light stimulation.

D. melanogaster data were acquired by Dr. S. Krause in 2006 (University of Oulu, Oulu, Finland). Preparation and patch-clamp recordings were performed as described previously (Krause et al., 2008). In contrast to *P. nivea* experiments, recording electrodes had a resistance of 12–15 MΩ, allowing whole-cell recordings with a series resistance of <20 MΩ. The bath solution was the same as above. Patch pipette solution contained (in mM) 140 KCl, 10 TES, 2 $MgCl_2$, 4 Mg-ATP, 0.4 Na-GTP, and 1 NAD, pH 7.15. The LJP in *Drosophila* experiments was −4 mV. All voltage values cited in the text were corrected for the LJPs. The series resistance was compensated by 80%. Recordings were performed at room temperature (21–22°C).

Data analysis

To evaluate photoreceptor performance, a white-noise contrast-modulated light stimulus was used (Frolov et al., 2017). The stimulus consisted of 30 repetitions of a 2-s Gaussian randomly modulated sequence, with a mean contrast of 0.36 and a corner frequency of 50 Hz, preceded by an adapting 1 s steady light. Responses to the stimulus were analyzed using Matlab 7.5 (MathWorks). All 2-s sequence response repeats were averaged in the time domain yielding a 2-s signal trace, which was consequently subtracted from each individual 2-s response to get noise traces, spectra of which ($N(f)$) were also averaged. The signal gain $T(f)|$ was calculated by dividing the cross-spectrum of photoreceptor input $C(f)$ and output $S(f)$ (photoreceptor signal) $S(f)\cdot C^*(f)$ by the autospectrum of the input $C(f)\cdot C^*(f)$ and taking the absolute value of the resulting frequency response function

$$T(f) = \frac{S(f)\cdot C^*(f)}{C(f)\cdot C^*(f)}.$$

The signal-to-noise ratio (SNR) was calculated as $S(f)/N(f)$, and the information rate was obtained using the Shannon equation in the frequency range of 1–50 Hz as

$$IR = \int_{1}^{50} log_2\left(\frac{|S(f)|}{|N(f)|} + 1\right) df.$$

Statistics

During statistical analysis, the Shapiro-Wilk normality test was first applied to data samples to determine if parametric statistical tests can be used. All experimental samples in this study have passed the normality test and were analyzed with parametric statistical methods as indicated. Data are presented as mean ± SD. Spearman's rank order correlation coefficient (SROCC, ρ) was used in analyses of correlations. Throughout the text, *n* stands for experimental group size.

Results

IA inhibition by 4-aminopyridine (4-AP) in *P. nivea*

As described in the previous study, photoreceptors in *P. nivea* express two Kv currents: a strong transient IA and a relatively small IDR (Frolov et al., 2017). To determine the role of IA in photoreceptor functioning, I first attempted to abolish IA pharmacologically while leaving IDR intact. In *D. melanogaster*, IA can be selectively blocked by 1 mM 4-AP (Elkins and Ganetzky, 1988), with similar results also obtained in *P. americana* (Salmela et al., 2012). I tested if 4-AP could block IA in *P. nivea*. Although 1 mM 4-AP could strongly reduce IA, complete suppression was usually observed at higher concentrations. However, concentrations above 2 mM often additionally reduced both IDR and light-induced current (LIC), which was undesirable. Therefore, 2 mM 4-AP was used, and all photoreceptors where this concentration reduced IA by less than 85%, or notably affected IDR or LIC, were discarded from the analysis. Fig. 1, A and B, demonstrates a typical example of IA inhibition. The effect of 4-AP was reversible (Fig. 1 C). On average, 2 mM 4-AP suppressed IA by ∼90% in the photoreceptors used for analysis (Fig. 1 D).

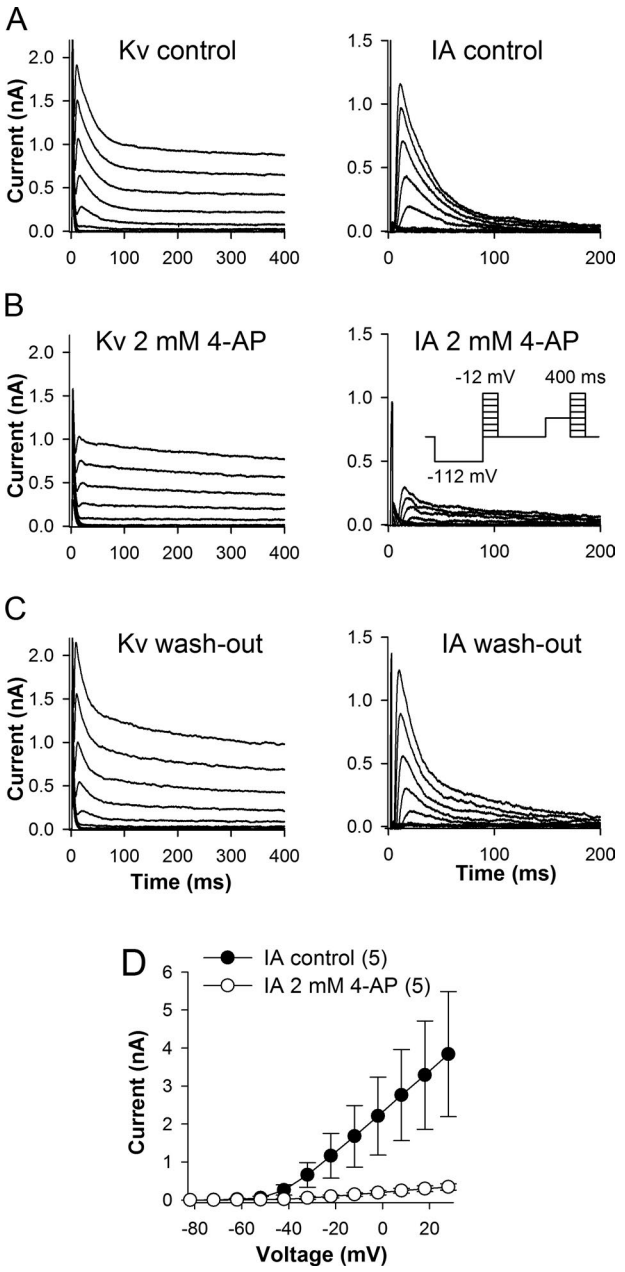

Figure 1. **Inhibition of IA with 4-AP in *P. Nivea*.** Delayed rectifier and transient K⁺ currents were recorded in the same *P. nivea* photoreceptor in control (A), after inhibition of IA with 2 mM 4-AP (B), and after washout (C), from an HP of −92 mV using a protocol displayed in the inset in the middle row. IA was obtained by subtracting current traces evoked by the second part of the protocol from the traces evoked by the first part. Current traces are shown for the voltage range of −72 to −12 mV. (B) Voltage-current relations for IA in control and after application of 2 mM 4-AP; here and elsewhere, error bars represent mean ± SD.

Effects of IA inhibition on voltage responses and information rates in *P. nivea*

Voltage responses and information processing were evaluated using a 61-s stimulus consisting of an adapting 1-s prepulse followed by 30 repeats of a 2-s Gaussian noise sequence with a corner frequency of 50 Hz (Gaussian white-noise [GWN] stimulus) Also, a 60-s naturalistic contrast-modulated light stimulus (NS) was used. Fig. 2, A and B, shows voltage responses of the same photoreceptor to the GWN stimulus presented at three light levels in 10-fold increments before and after inhibition of IA. Fig. 2 C shows responses of the same photoreceptor to a moderately bright NS in control and after inhibition of IA. Application of 4-AP did not alter the resting potential (data not shown). There was no significant effect of application of 2 mM 4-AP on membrane depolarization during light responses (Fig. 2 D).

Information rates were calculated from SNR functions (see Methods). Typical signal and noise traces at a relative light intensity (RLI) of 10^{-2} before and after application of 2 mM 4-AP are shown in Fig. 3 A. Kv currents recorded in this photoreceptor are shown in Fig. 1, A–C, and voltage responses in Fig. 2, A and B. It can be seen that both signal and noise traces before and after application of 4-AP are nearly identical. Consistently, only marginal differences could be seen between signal gain and SNR functions under two conditions (Fig. 3, B and C; data correspond to traces in Fig. 2, A and B). On average, information rates were not significantly different (Fig. 3 D). Corner frequencies were obtained by fitting the voltage dependencies of signal gain with a first-order

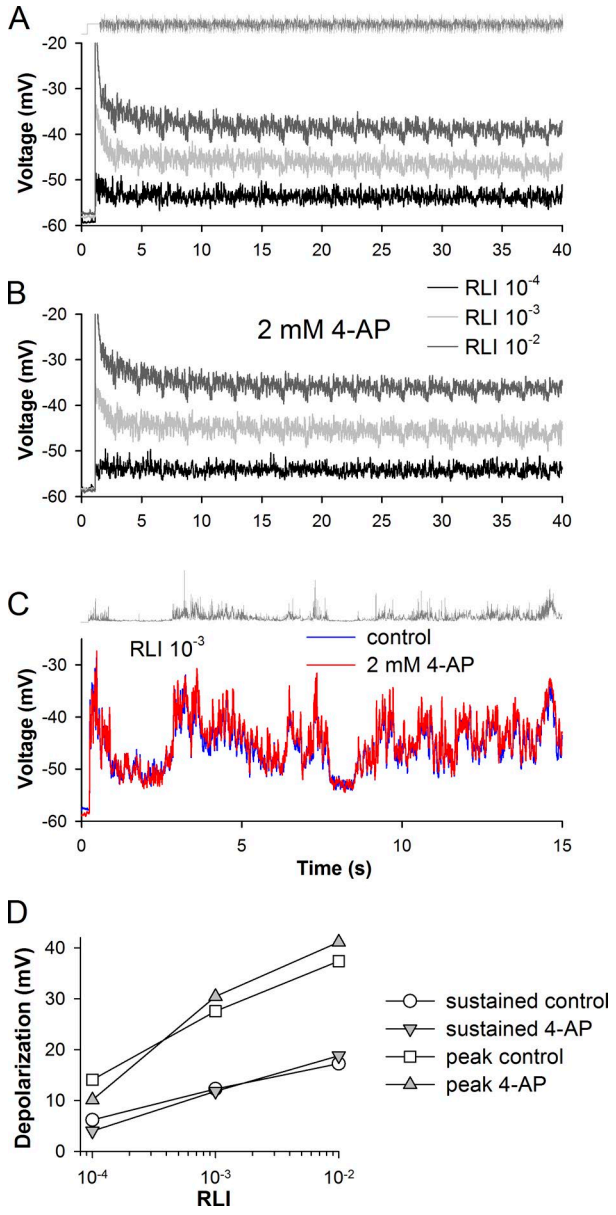

Figure 2. **Effects of 2 mM 4-AP on voltage responses. (A and B)** Voltage responses to GWN stimulus from the same photoreceptor in control (A) and after inhibition of IA (B) at three light levels in tenfold increments; the stimulus (gray trace above the responses) is shown in A. In this and following figures, the maximal RLI of 1 approximately corresponds to bright room illumination and, when used for stimulation, in most cases irreversibly degrades in vitro photoreceptor responses. **(C)** Superposition of responses to NS before and after inhibition of IA in the same photoreceptor as in A and B; the responses were obtained at intermediate RLI of 10^{-3}. **(D)** Dependence of the peak and sustained depolarization on light intensity before and after inhibition of IA for the photoreceptor in A; sustained depolarization was determined by subtracting resting potential value from the average plateau potential between 3 and 61 s after the onset of light stimulus.

Lorentzian function. Apparent inhibition of IA had no effect on corner frequency (Fig. 3 E).

IA and elementary responses in *P. nivea*

Because IA in *P. nivea* was characterized by low activation threshold, HAP, and relatively large window current, IA was expected to be essential for shaping elementary responses. Therefore, I compared voltage bumps evoked in dim light in control and after application of 4-AP. Fig. 4 A shows recordings in the same photoreceptor before and after inhibition of IA. No significant differences could be discerned. Since voltage bump amplitude and kinetics are strongly affected by momentary conductance and membrane capacitance, the experimental groups were controlled for membrane potential and capacitance (unpaired groups: −61.6 ± 3.9 mV/282 ± 22 pF in control, and −62.0 ± 3.2 mV/293 ± 61 pF after IA block). On average, voltage bumps were not affected by inhibition of IA (Fig. 4 B). Likewise, IA block did not alter current quantum bumps recorded in steady dim light by voltage clamp (Fig. 4 C).

Analysis of physiological variability

Experiments with pharmacological blockade had several important shortcomings. Assuming that 4-AP inhibits IA via open-channel block, such a mechanism requires that the channel opens first and presents the drug binding site in the pore to the blocker molecule (Frolov and Singh, 2014). This results in a residual conductance, the size of which depends on the frequency and magnitude of stimulation. Furthermore, open-channel blockade is usually voltage dependent, with stronger current suppression observed at more depolarized voltages where channels stay longer in the open state, whereas the upper boundary of physiological depolarization during sustained signaling in microvillar photoreceptors rarely exceeds −30 mV in vitro. Moreover, it is difficult to determine IA at voltages near its activation threshold, where the current is small, due to a small driving force for K^+ ions, and is predominantly noninactivating. The presence of other sustained currents, including IDR, chloride, and the genuine leak current, together with the instrumental leak current, preclude reliable isolation of IA. Collectively, these uncertainties do not allow establishment of the role of IA in dim light backgrounds using only experiments with 4-AP.

In the following experiments, voltage responses to GWN were recorded from 27 green-sensitive photoreceptors at several light levels in 10-fold increments, ranging from RLI of 10^{-5} to 10^{-1} depending on the light sensitivity of individual photoreceptors. However, usually only three light levels were used (Fig. 2 A), with the dimmest GWN producing a response characterized by low depolarization, low information rate, and high noise, whereas the response to the brightest GWN usually exhibited signs of saturation, e.g., a progressive decrease in response variance. Group-average changes in photoreceptor performance with light level are presented in Fig. 5. Fig. 5 A shows dependence of sustained depolarization on stimulus brightness. Membrane corner frequency decreased linearly with increasing stimulus intensity (Fig. 5 B) or the accompanying depolarization (Fig. 5 C). Despite the decrease in f_{3dB}, the mean information rate increased up to RLI of 10^{-2}, after which the photoreceptor signal deteriorated (Fig. 5 D).

I hypothesized that as amplitudes and voltage dependencies of IA and IDR vary between photoreceptors (Fig. 6, A and B), the associated changes in information processing might help determine the functions of the currents. Hypothesizing that large early conductance could facilitate transfer of higher signal

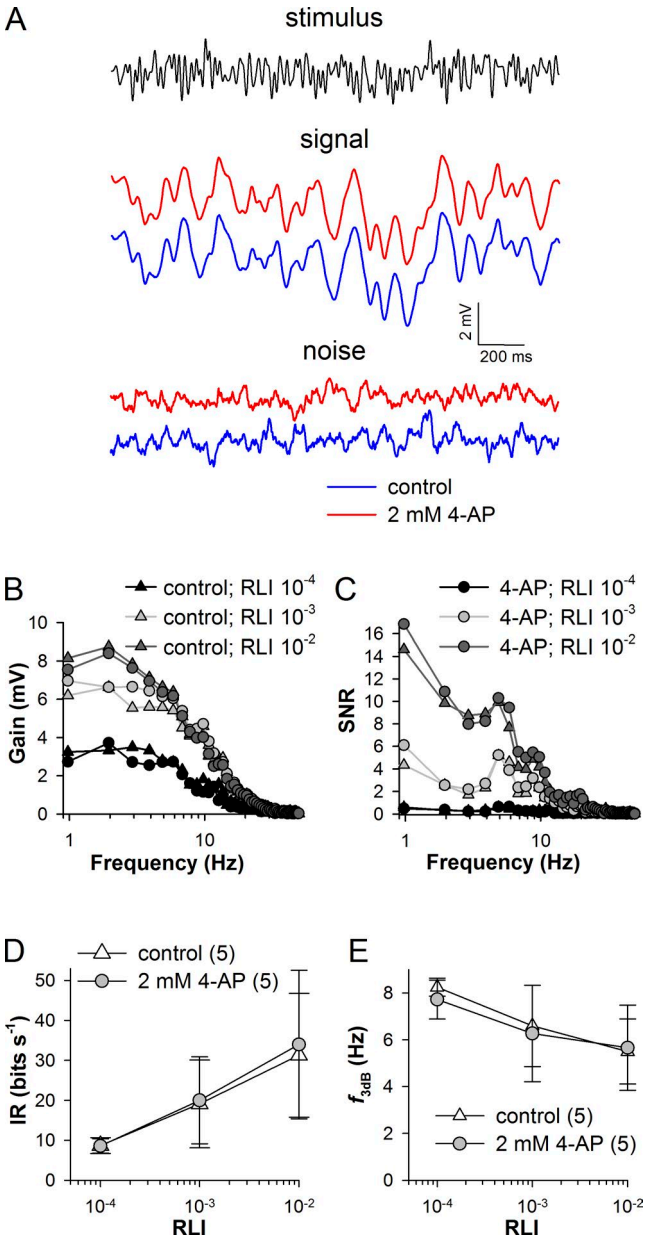

Figure 3. **Inhibition of IA by 4-AP does not affect signal processing in *P. nivea* in moderate and bright light. (A)** 2-s signal and noise traces in control and after inhibition of IA were recorded in the same photoreceptor, with the stimulus shown in black; the signal was obtained by averaging 30 response repeats from the 60-s voltage response to GWN at the RLI of 10^{-2}. **(B and C)** Voltage signal gain (B) and SNR (C) functions in control and in the presence of 2 mM 4-AP obtained from responses in Fig. 2, A and B; in both panels, triangles denote control and circles denote the presence of 4-AP (the legend to symbols is divided between the two panels). **(D and E)** Mean information rates (D) and the corresponding corner frequencies (E) at three light levels before and after application of 2 mM 4-AP; f_{3dB} values were obtained from gain functions by fitting them with a first-order Lorentzian function; data from the same five photoreceptors. IR, information rate.

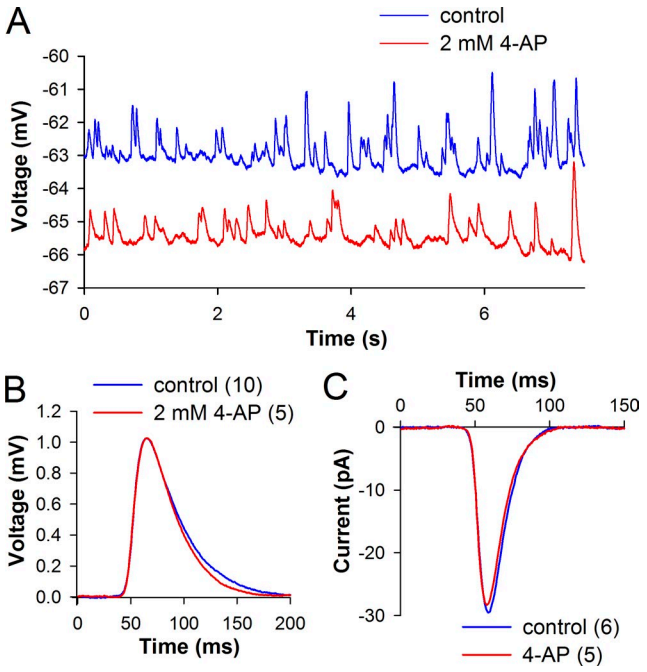

Figure 4. **4-AP does not affect elementary voltage responses. (A)** Voltage bump responses in steady dim light from the same photoreceptor before and after application of 2 mM 4-AP. **(B)** Mean voltage bumps were produced from unpaired recordings in control and after IA inhibition; group averages were obtained in the following way: first, mean bumps were obtained for each photoreceptor; second, a subsample of photoreceptors was selected so that their mean resting potentials were nearly the same for the two experimental conditions. **(C)** Mean current bumps were not altered in the presence of 2 mM 4-AP; bumps were evoked by 1-ms flashes of low-intensity light from a HP of −82 mV; mean bumps were determined for each photoreceptor, and then group averages were obtained.

frequencies, peak IA and sustained IDR amplitudes at different membrane potentials were correlated to f_{3dB} values obtained from responses to GWN at three backgrounds, RLI 10^{-4} to 10^{-2}. Fig. 6 C shows dependencies of the correlations for IA on membrane potential. A clear maximum can be seen at −52 mV, which corresponds to the maximal IA window current (see Fig. 7 E in Frolov et al., 2017). Two correlations shown in Fig. 6 D illustrate these findings. The highest SROCC of 0.73 was observed in the dimmest 10^{-4} background, which is consistent with greater availability of IA channels at this than at more depolarizing 10^{-3} and 10^{-2} backgrounds. IDR amplitudes also correlated positively with the corner frequencies, but the correlations were comparatively weak and increased with membrane depolarization, except at the 10^{-4} background, where the maximal correlation of 0.56 was found at −42 mV (Fig. 6 E).

A similar analysis was performed using HAPs for IA and IDR as proxies for the current amplitudes. A low HAP reflects an early activating current and vice versa. HAP values were obtained by fitting conductance-voltage relations with a Boltzmann's charge-voltage equation (Fig. 7, A and B). On average, HAP was −32.8 ± 8.2 mV for IA and −35.3 ± 6.6 mV (n = 27) for IDR. Variability in HAP was greater for IA than IDR (Fig. 7, A and B). There was a moderate positive statistically significant correlation between HAP values for two currents (Fig. 7 C). Statistically significant negative correlations were found between HAP for IA and f_{3dB} at RLIs from 10^{-4} to 10^{-2} (Fig. 7, D and F). Interestingly, HAP for IDR correlated significantly with f_{3dB} at RLIs of 10^{-4} but not in brighter backgrounds (Fig. 7, E and F). However, even in the relatively dim background of 10^{-4}, the correlation was stronger for IA than for IDR (Fig. 7, D–F). The information rate correlated

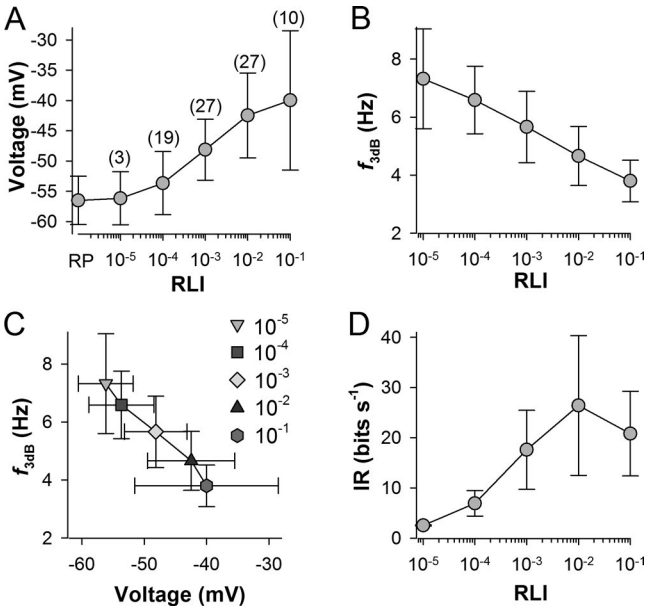

Figure 5. **General properties of responses to GWN. (A)** Mean sustained membrane depolarization at different light levels during responses to GWN; numbers stand for the number of photoreceptors at each background in A–D; RP, resting potential (n = 27). **(B and C)** Changes in membrane corner frequency with light level (B) and the associated depolarization (C). **(D)** Changes in information rates.

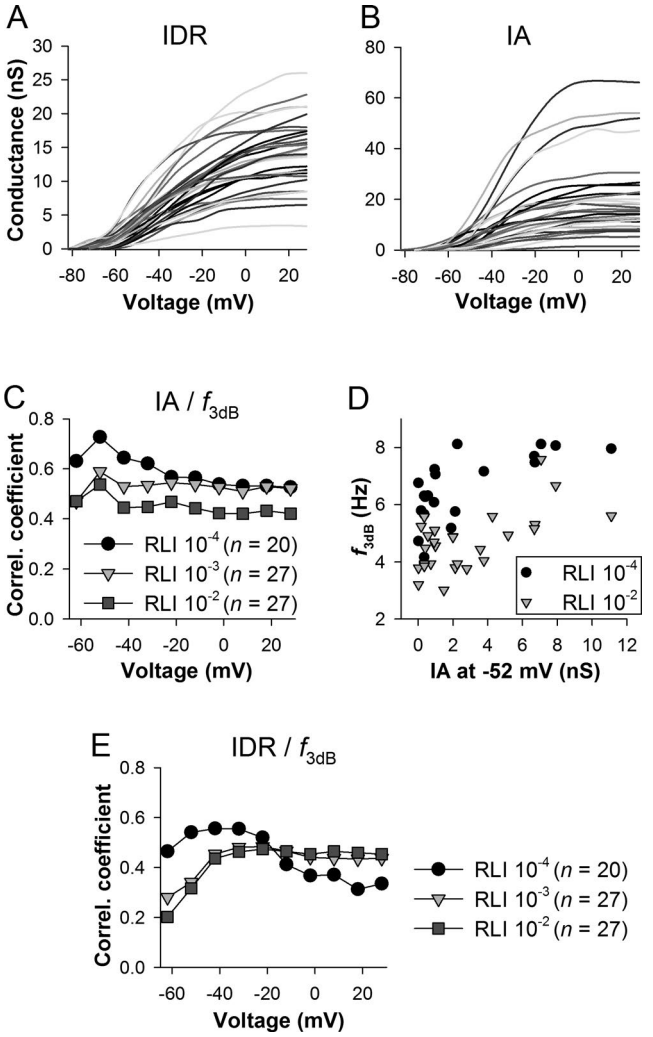

Figure 6. **Correlations (Correl.) between IA and IDR amplitudes and corner frequency. (A and B)** Conductance-voltage relations for IDR (A) and peak IA (B) were obtained from 27 photoreceptors. At each voltage in the range from −62 to +28 mV, the correlations between IA and IDR conductance, on the one hand, and corner frequencies at RLIs of 10^{-4}, 10^{-3}, and 10^{-2}, on the other hand, were measured using SROCC. **(C)** Voltage dependencies of correlation coefficients for IA/f_{3dB} correlations; P < 0.03 for all correlations. **(D)** Examples of two correlations for IA at −52 mV at RLI of 10^{-4} and 10^{-2}. **(E)** Voltage dependencies of correlation coefficients for IDR/f_{3dB} correlations; at RLI of 10^{-4}, P < 0.04 for voltages −62 through −22 mV; at RLIs of 10^{-3} and 10^{-2}, P < 0.03 for −42 mV and all more positive voltages.

strongly with f_{3dB} in the bright 10^{-2} background but not at dimmer light levels (Fig. 7 G). These results suggest that IA facilitates transfer of higher-frequency signals.

What mechanism could cause the expansion of signaling bandwidth by IA? Graded voltage response is a superposition of transient bump-like voltage responses. It is possible that the fast-activating IA decreases the speed of membrane charging and relaxation by reducing the momentary membrane time constant, and through this facilitates resolution of individual responses. Fig. 8 shows examples of mean voltage bumps evoked by continuous dim light at resting potential in six photoreceptors characterized by different membrane capacitance and HAP for IA values. Since the input resistance crucially depends on membrane potential, the recordings were arbitrarily combined into two groups with similar resting potentials as indicated. It can be seen that photoreceptors with more negative HAP values generate voltage bumps with faster onsets and smaller half widths than photoreceptors with more positive HAP for IA.

IA in *D. melanogaster*: Revisited

Electrophysiological studies addressing the role of IA in photoreceptors of *D. melanogaster* mainly relied on intracellular recordings in wild-type and *Shaker* null mutant flies (Sh^{KS133}; Juusola et al., 2003; Niven et al., 2003b). Two main findings that can be assessed in independent voltage-clamp experiments are (1) the nonlinear dependence of sustained membrane conductance in the dark on voltage, and (2) the increased leak conductance in Sh^{KS133} photoreceptors. The first effect was attributed to inactivation of Shaker channels and is crucial for the early nonlinear amplification hypothesis, whereas the second one is the foundation of the compensatory changes hypothesis.

Voltage-activated conductances were studied in patch-clamp recordings from photoreceptors in dissociated ommatidia from a wild-type *CS* and IA null mutant Sh^{KS133} strains. Fig. 9 A shows averaged current traces evoked in wild-type photoreceptors from a holding potential (HP) of −64 mV by 100-ms voltage pulses between −74 and +36 mV in 10-mV increments. Fig. 9 B shows averaged current traces recorded under the same conditions in Sh^{KS133} photoreceptors. Shaker IA can be obtained by subtracting currents in Fig. 9 B from the currents in Fig. 9 A. It can be seen that IA in *D. melanogaster* is much smaller than IA in *P. nivea* (Fig. 9 C). In *D. melanogaster*, values of HAP were −14.6 mV for IA and +11.9 ± 2.0 mV (n = 9) for IDR (current values at the end

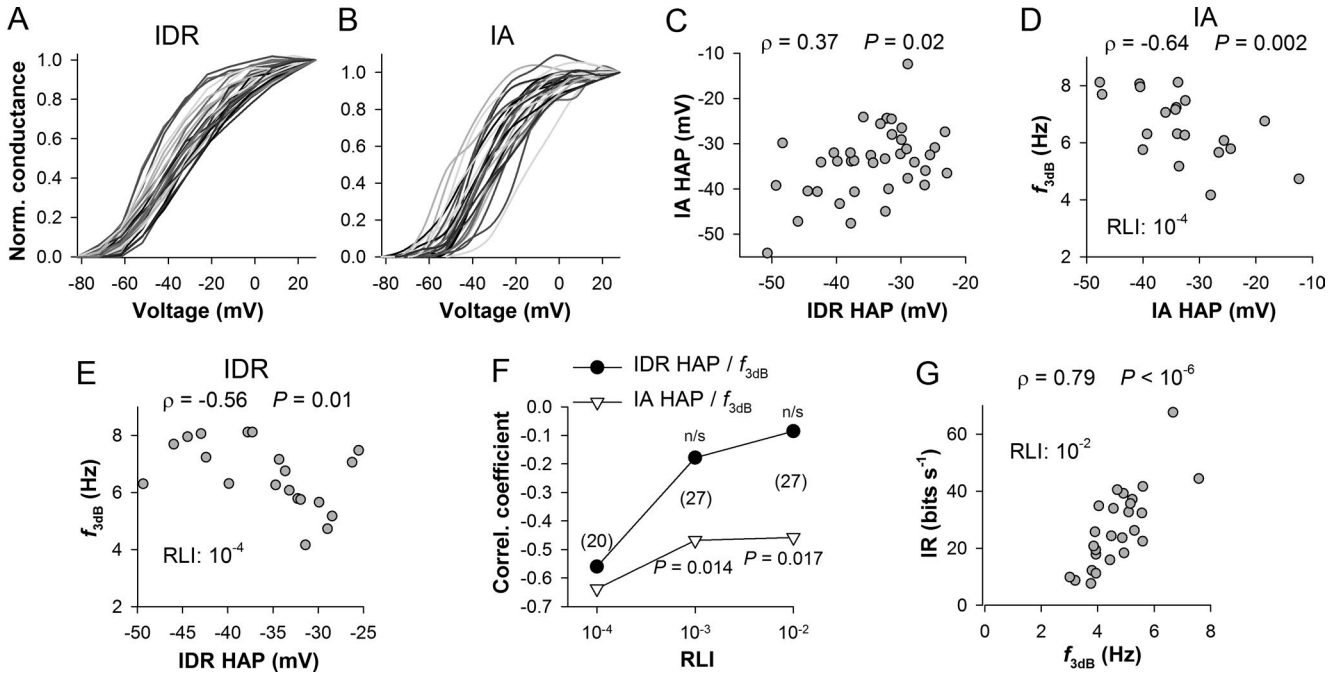

Figure 7. **HAPs and information processing. (A and B)** Normalized (Norm.) conductance-voltage relations for IDR (A) and peak IA (B); data from the same 27 photoreceptors as in Fig. 6, A and B. **(C)** Correlation (Correl.) between HAPs for IDR and IA; the correlation was statistically significant as indicated. **(D and E)** Correlations between HAPs for IA (D) or IDR (E) and corner frequency at RLI of 10^{-4}. **(F)** SROCC values for correlations between HAPs for IA or IDR and f_{3dB} at three backgrounds; numbers in parentheses indicate the number of cells; n/s, not significant. **(G)** Correlation between f_{3dB} and information rate at RLI of 10^{-2}.

of 100-ms pulses were used). Accordingly, the HAP for IDR in Sh^{KS133} photoreceptors was +11.0 ± 6.7 mV (n = 8).

The early nonlinear amplification hypothesis postulates that Shaker channels in *D. melanogaster* begin activating at around resting potential. At such negative voltages, they do not undergo inactivation and therefore underlie what is effectively a sustained K^+ conductance. Then, when the cell is depolarized by a few millivolts, inactivation of Shaker channels sets in, and the total membrane conductance decreases if the IDR activation threshold is not yet reached and Shab channels do not begin opening en masse. As a result, the amplitudes of small light-induced voltage responses at potentials slightly above rest become higher than similar responses evoked at the resting potential, where the effective IA conductance is higher. Two testable predictions follow from this: (1) the decrease in conductance upon small depolarization should be observed in wild-type but not in Sh^{KS133} photoreceptors, and (2) the decrease in conductance should be more prominent after prolonged depolarizations as IA inactivation is slow at such membrane potentials.

The results shown in Fig. 9, D and E, do not generally support the Shaker-based early amplification hypothesis. Fig. 9 D shows a prolonged 6-s Kv recording from a wild-type photoreceptor. Examining the current traces evoked by voltage pulses near the resting potential in the second half of the recording (colored traces inset) after subtracting the offset and scaled-up leak currents (the current between −74 and −64 mV was defined as leak) revealed that in this cell, the total voltage-activated K^+ conductance indeed decreases between −64 and −54 mV (blue and green traces). However, such a pronounced decrease in conductance was observed only in one out of five photoreceptors (Fig. 9 E, blue traces). Surprisingly, examination of prolonged recordings in Sh^{KS133} photoreceptors revealed that one out of three photoreceptors was also characterized by a decrease in conductance at −54 mV. Next, 100-ms recordings were examined (Fig. 9 F). It can be seen that a minority of photoreceptors from both wild-type and Sh^{KS133} groups were characterized by decreasing conductance between −54 and −44 mV. This was observed in photoreceptors where the activation threshold for IDR was especially high (Fig. 9, E and F). On average, the current at the end of 100-ms voltage pulses between −44 and −24 mV was significantly larger in wild-type than *Shaker* photoreceptors ($P < 0.007$ at all three potentials; Fig. 9 G). However, the differences became statistically insignificant at the end of 6-s responses (Fig. 9 H).

Intracellular recordings in Sh^{KS133} photoreceptors were characterized by a relatively large leak conductance, which was interpreted as a compensatory development (Niven et al., 2003a). If this leak conductance is mediated by ion channels expressed in the soma, it would manifest in whole-cell patch-clamp recordings as well. However, comparative analysis of leak current in control and Sh^{KS133} flies showed that the total leak conductance, which consists of the instrumental and physiological leak conductances, was not significantly different between the experimental groups: at the end of 100-ms voltage pulses between −74 and −64 mV, the leak conductance equaled 1.05 ± 0.58 nS in control (n = 9) versus 0.69 ± 0.37 nS in Sh^{KS133} photoreceptors (n = 8).

Discussion

In this work, I investigated the role of IA in signal processing in *P. nivea* photoreceptors and reexamined the situation in *D. melano-*

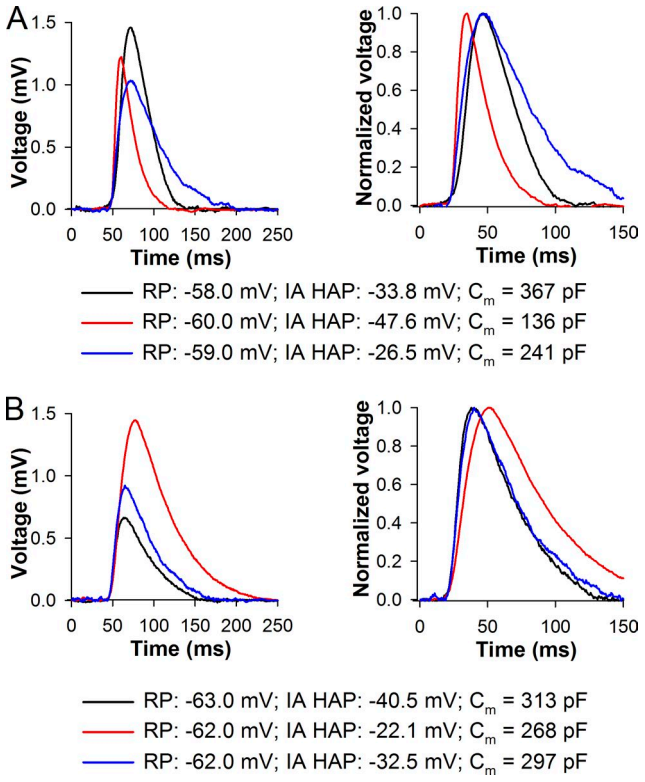

Figure 8. **Voltage bumps in photoreceptors with different HAP for IA.** Voltage bumps were evoked by dim continuous light from resting potential; mean voltage bumps for each photoreceptor are shown. C_m, membrane capacitance; RP, resting membrane potential. **(A)** Mean voltage bumps in three photoreceptors with resting potentials between −58 and −60 mV. Here and in B, the original mean bumps are shown to the left, and normalized bumps to the right. **(B)** Mean bumps in three photoreceptors with resting potentials between −62 and −63 mV.

gaster. I found some evidence for IA involvement in conditioning voltage responses in *P. nivea*, whereas the findings in *D. melanogaster* were inconsistent with the long-standing hypotheses on the role of IA (Juusola et al., 2003; Niven et al., 2003a,b).

The problem of IA is complex and needs to be separated into three distinct subproblems: (1) Why do photoreceptors need a rapidly activating Kv conductance, (2) what is the utility of a rapidly inactivating Kv conductance, and (3) what is the use for IA as it is—a rapidly activating and inactivating current?

The first question was addressed previously in several comparative studies, and it appears that having a large, fast-activating conductance is a prerequisite for fast vision (Weckström and Laughlin, 1995; Frolov et al., 2016). However, such current can play a dual role. The first one would be counteracting similarly fast high-frequency LIC transients and attenuating high-frequency signals and noise. On the other hand, by rapidly increasing membrane conductance and thus decreasing the momentary membrane time constant, it should facilitate transfer of high-frequency signals by preventing their excessive low-pass filtering. This effect would be more salient in the vicinity of resting potential, where the driving force for K^+ ions is relatively small and the opening of fast-activating Kv channels would not elicit a strong counteracting repolarizing current while providing a substantial conductance. Although in this situation, the conductance can also be expected to reduce the gain of high-frequency signals, the efficiency of the signal transfer is eventually determined at the first synapse. The synapse, however, appears to be a dynamically adapting differentiating device, which emphasizes transmission of fast over slow components of the graded signal (Juusola et al., 1995; Baden et al., 2013), thus favoring the high-frequency facilitation function. Consistently, here I demonstrated that in *P. nivea* photoreceptors, the signal transfer bandwidth as measured by membrane corner frequency is proportional to the amplitude of IA.

The utility of a rapidly inactivating Kv conductance was also studied previously in several species (Cuttle et al., 1995; Weckström and Laughlin, 1995; Laughlin, 1996). The current opinion is that it helps preventing unnecessary metabolic expenses and suppresses high-frequency noise.

The answer to the third question is probably related to the lifestyle and behavior of the species. *P. nivea* is a nocturnal species, and *D. melanogaster* is also mainly active during low light periods. If strong photoreceptor depolarizations occur infrequently and briefly in these and similar species, then it might be sufficient for them to express a fast-activating and -inactivating Kv conductance rather than a fast-activating sustained conductance such as found in diurnal blowflies (Weckström et al., 1991).

IA in *P. nivea*

The experiments in *P. nivea* consisted of two parts: acute pharmacological inhibition of IA with 4-AP and analysis of normal variability in a relatively large group of photoreceptors. While the tests with 4-AP allowed rapid removal of IA with immediate registration of associated effects, such results could be interpreted with confidence only for fairly depolarized responses. Due to the uncertain extent of IA blockade in the lower half of the physiological voltage range, i.e., 10- to 15-mV depolarization from the resting potential, the absence of changes in photoreceptor signaling in relatively dim backgrounds cannot be interpreted as the absence of IA function. On the other hand, during stimulation with bright GWN, which elicits relatively highly depolarized sustained responses, most of IA can be expected to be removed by inactivation (see voltage dependence of IA inactivation in Fig. 7 E of Frolov et al., 2017). Use of 4-AP in such circumstances might add little to that removal. The variability analysis was based on the premise that if amplitudes of Kv currents differ from cell to cell in the physiological voltage range, then the accompanying variability in the higher photoreceptor functions might help to explain the roles of the currents. In this analysis, both direct conductance and indirect HAP values were used as measures of the currents.

There are several possible functions or electrophysiological situations where IA could improve photoreceptor signaling. First, by rapidly increasing membrane conductance and decreasing the membrane time constant, IA could accelerate the initial transient depolarizing responses of dark-adapted photoreceptors stimulated by relatively bright light. However, neither the experiments with 4-AP described here nor the previous modeling study in *P. americana* (Salmela et al., 2012) support this function. There was no detectable effect of IA removal on the amplitude, width, or onset kinetics of the large initial depolarizing transient.

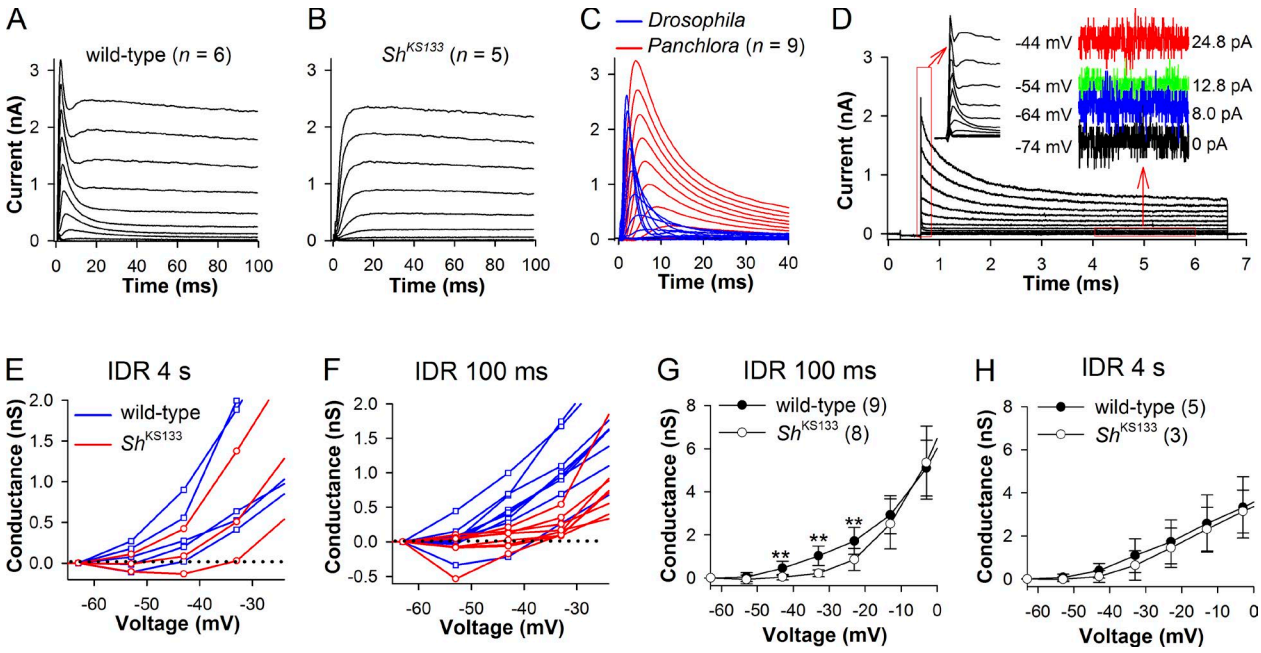

Figure 9. **Voltage-activated K⁺ conductances in *D. melanogaster* photoreceptors. (A)** Voltage-activated K⁺ current in wild-type *D. melanogaster* was recorded from an HP of −64 mV using 100-ms voltage pulses applied in 10-mV increments from −74 to +36 mV; each pulse was preceded by a 100-ms pulse to −104 mV to recover IA from inactivation; the traces are averages of recordings from six photoreceptors. **(B)** Averaged (n = 5) current traces from the *Shaker* mutant obtained as in A. **(C)** Comparison of IA in *D. melanogaster* and *P. nivea*; *D. melanogaster* IA was acquired by subtracting traces in B from the traces in A; *P. nivea* IA is the average of currents from nine photoreceptors obtained as in Fig. 1 A. **(D)** Prolonged 6-s recordings of Kv current in wild-type *D. melanogaster* photoreceptors; the current was recorded as in A with a 400-ms prepulse to −104 mV. Inset left shows the IA. Inset right shows four current traces elicited by voltage steps between −74 and −44 mV as indicated; the average current value at −74 mV was subtracted from all traces; the corresponding resulting average current values are shown at right. **(E)** Conductance-voltage relations for sustained IDR currents in wild-type and *Shaker* photoreceptors in the voltage range between −64 and −24 mV; current values were obtained by averaging currents between 4 and 6 s after the onset of voltage steps; leak conductance was determined between −74 and −64 mV and subtracted from all traces; black dotted line indicates zero conductance. **(F)** Conductance-voltage relations for IDR between 70 and 100 ms after the onset of voltage steps. **(G)** Average conductance-voltage relations for IDR from F. In wild-type photoreceptors, IDR was significantly higher than in *Shaker* photoreceptors at three potentials as indicated. **(H)** Average conductance-voltage relations for IDR from E.

This might be explained by the relatively slow onset and large half width of the transients evoked by flashes of bright light, as IA channels would be strongly inactivated by the time the peak of the transient is reached. However, it should be noted that the transients seem to be consistently slower and wider in patch-clamp than in intracellular recordings (data not shown), probably because of the absence of additional conductances associated with either the axon or the instrumental leak due to membrane piercing (see below), so that a role for IA in modulating the transient in vivo cannot be ruled out.

However, the most likely function for IA is the facilitation of transfer of high-frequency components of the stimulus by modulating small-voltage transients that form the sustained light response (Fig. 8). Strong and statistically significant correlations found between the measures of IA and f_{3dB} values (Figs. 6 and 7) are consistent with this hypothesis. Notably, the strength of the correlations between HAP for IA and f_{3dB} decreased in brighter backgrounds consistently with the progressive inactivation of IA with increasing membrane depolarization (Fig. 7 F; see also Fig. 7 E in Frolov et al., 2017). Interestingly, correlations between the actual IA conductance values and f_{3dB} were voltage dependent, with the strongest one observed precisely at the voltage linked to the maximal IA window current, −52 mV (Fig. 6 C). The correlations decreased steadily as the membrane was further depolarized, pointing to a growing disconnect between the peak IA conductance at each membrane potential determined in voltage-clamp experiments and the actual persistent IA during sustained voltage responses to GWN.

The strongest correlations between the actual IDR conductance values and f_{3dB}, and also between HAC for IDR and f_{3dB}, were found in the relatively dim light, at RLI of 10^{-4} (Figs. 6 E and 7 F). What could explain this finding? As the level of sustained depolarization is determined by the balance between depolarizing LIC and repolarizing Kv conductances, in relatively bright light, the level of depolarization is set by the interplay between LIC and IDR since IA is mostly inactivated. Bright light activates a sufficiently large IDR conductance as not to restrict the signaling bandwidth (or to restrict it to a similar degree in cells with different HAP for IDR). In contrast, both IA and IDR are likely to be involved in repolarization in relatively dim light so that the correlation between HAP for IDR and f_{3dB} at RLI of 10^{-4} could reflect the differences in IDR activation thresholds between photoreceptors.

Examination of individual voltage bumps in similar physiological variability analysis could possibly reveal the electrophysiological mechanisms by which IA and IDR influence membrane corner frequency. However, a much larger experimental dataset would be needed to achieve this goal than currently available because there are many factors modulating elementary voltage responses, such as membrane capacitance, conductance and HAP values for IA and IDR, quantum bump amplitude and latency, etc.,

Table 1. **Mean HAP values for IA and IDR in insect photoreceptors with a prominent IA (see Frolov et al., 2016).**

Species	HAP, mV		IDR at −40 mV, nS	IDR at −40 mV, pS/pF	Reference
	IA	IDR at 400 ms			
Carausius morosus	−12.4 ± 2.0	−23.2 ± 1.9	2.5	21	Frolov et al., 2012
Corixa punctata	−25.5 ± 7.9	−25.7 ± 7.3	6.6	15	Frolov, 2015
D. melanogaster	−14.6[a]	+2.7 ± 9.4	1.1	20[b]	Fig. 9
D. virilis	−22.4 ± 5.9	−27.5 ± 2.5[c]	9.0[c]	106[c]	Not published
Gerris lacustris	−19.0 ± 6.0	−18.0 ± 10.0	3.3	57	Frolov and Weckström, 2014
Gryllus bimaculatus	−20.5 ± 3.8	−22.1 ± 11.2[d]	5.2	46	Frolov et al., 2014
P. nivea	−34.6 ± 7.4	−34.5 ± 7.1	5.3	20	Frolov et al., 2017

[a]From the current traces in Fig. 9 C.
[b]Average photoreceptor capacitance value of 55 pF was used (Frolov, 2016). *D. virilis* values were obtained from unpublished data.
[c]At the end of 100 ms pulses; the average capacitance value of 85 pF was used (Frolov, 2016).
[d]For regular green-sensitive photoreceptors in dark-adapted crickets (Frolov et al., 2014).

and their effects need to be explored while controlling membrane potential as strictly as possible.

IA in *D. melanogaster*

Despite the differences in activation ranges of IA and IDR between *D. melanogaster* and *P. nivea*, sustained voltage responses in bright light in both species are mostly counteracted by IDR, and it follows from the results in *P. nivea* that IA can hardly affect information transfer in bright light. How can this be reconciled with findings in *D. melanogaster*, where *Shaker* null mutant flies exhibited strongly decreased information capacity across the entire range of light intensities (Niven et al., 2003b)? Apparently, the reduction in information capacity, especially in bright light where IA should be completely inactivated, cannot be caused by the loss of IA conductance per se. In general, differences between wild-type and mutant phenotypes can arise from multiple sources, including the effects of the mutation, the accompanying physiological compensatory changes, differences in genetic backgrounds, and interactions between the background and the gene of interest (Linder, 2006). Moreover, the functions of a gene are not always limited to the function of its namesake protein (see, e.g., Gomez-Ospina et al., 2013). In the *D. melanogaster* study, the changes in the mutant photoreceptors had all the hallmarks of a highly increased leak conductance as the underlying cause: reduced response variance and voltage gain, reduced impedance in the lower frequency region, and increased membrane corner frequency (Niven et al., 2003b).

In the following study, when the additional leak conductance found in *Shaker* null mutants was incorporated into a mathematical model, the resulting metabolic cost of visual information processed by photoreceptors increased twofold (Niven et al., 2003a). The increased leak was considered a necessary developmental compensation for the absent IA, and it was concluded that expression of Shaker channels reduces the cost of information. However, increased leak current in *Shaker* null mutants is a strong confounding factor, altering the whole electrophysiological phenotype of the mutant photoreceptors. No valid conclusion on the specific electrogenic function of Shaker channels, such as their putative involvement in information processing or energy metabolism, is possible without separating the effects of IA knockout from those of the increased leak. Moreover, increased leak might not be the only compensatory development in the mutant, as changes in light-induced conductance were proposed in the subsequent study by the same authors (Niven et al., 2004). This problem needs to be addressed in future experimental studies.

It should be noted that a similar increase in leak current was found in the study of small conductance Ca^{2+}-activated K^+ channels in *D. melanogaster* photoreceptors (Abou Tayoun et al., 2011), indicating that it is a nonspecific development. Its origin remains unclear, and here I provided evidence that the leak current in *Shaker* photoreceptors at the level of the soma does not exceed that in wild-type photoreceptors. This suggests that it might be caused by changes in the axon, i.e., in the presynaptic terminal.

Finally, IA was proposed to amplify relatively small voltage responses to light at potentials slightly above the resting potential (Juusola et al., 2003; Niven et al., 2003b). While it cannot be contested that transition of Shaker-based IA from a persistent to inactivating conductance with progressive membrane depolarization would increase membrane resistance if IA was the only voltage-dependent conductance in the cell, in practice the situation is more complex because photoreceptors express several voltage-dependent channels. Due to natural variation in the amplitudes and voltage dependencies of such conductances, Shaker can be expected to amplify voltage signals only under specific conditions, when a decrease in IA with depolarization is not offset by opening of other channels. Indeed, results presented here indicate that the decrease in conductance with increasing membrane potential is a valid phenomenon. However, it was observed only in a minor fraction of photoreceptors characterized by a high activation threshold for IDR. According to Fig. 9, E and F, the total conductance could decrease by as much as 0.5 nS; considering that the average leak conductance is ∼1 nS, such a 0.5-nS decrease can lead to a noticeable low-frequency amplification of voltage responses. Furthermore, as some of the leak conductance is probably caused by the imperfect electrode-membrane seal interface, the actual amplifi-

cation might be even stronger. However, since the decreasing conductance was found in equal measure both in control and Sh^{KS133} photoreceptors, it cannot be plausibly attributed to IA only. The question of amplification has been revisited by the same authors in the upcoming modeling study in *D. melanogaster* (Heras et al., 2018), who suggest that amplification has no real function, and the main function of the Shaker conductance is through activation to increase bandwidth at low light levels.

D. melanogaster as an outlier

Recent comparative electrophysiological studies of microvillar photoreceptors imply that the very positive HAP for IDR found in *D. melanogaster* is an exception rather than a typical situation. Table 1 compares some properties of IA and IDR in seven species characterized by a prominent IA current, including a *D. melanogaster* relative, *D. virilis*. In all cases except *D. melanogaster*, HAPs for IDR were equal or more negative than the HAPs for IA. (However, it should be noted that the utility of the HAP concept is limited because it strongly depends on the inactivation state of the channel pool: for instance, in the photoreceptor shown in Fig. 9 D, the nominal value of the momentary HAP decreases from +14 mV at 100 ms after the onset of voltage steps to 0 mV between 4 and 6 s due to a disproportional inactivation of IDR at positive voltages.) As a consequence of such a positive HAP for IDR in *D. melanogaster*, IDR conductance in the lower part of the physiological voltage range (in Table 1, an arbitrary value of −40 mV was used) was smallest in the fruit fly. However, if instead of conductance per se, IDR conductance densities (conductance divided by capacitance) were estimated, then *D. melanogaster* cannot be considered an outsider. The IDR conductance density value has been linked to visual ecological and behavioral traits of the species (Frolov, 2016). Although the reason for such an unusual arrangement of Kv conductances in photoreceptors of *D. melanogaster* is not clear, the difference between the HAPs is not fixed and subject to modulating influences capable of eliminating the difference altogether as it was shown previously (Hevers and Hardie, 1995).

Conclusions

Results presented here suggest that IA might play the same roles in both *D. melanogaster* and *P. nivea* photoreceptors, i.e., facilitating transmission of high-frequency signals. In *D. melanogaster*, discovery of this function was probably obfuscated by the increased membrane corner frequencies in the *Shaker* null mutant clearly caused by high leak conductance (Niven et al., 2003b; Heras et al., 2018). On the one hand, such compensatory developments in mutants lacking important proteins limit utility of the mutational analysis. On the other hand, pharmacological inhibition can be unreliable, as exemplified in this study. Combining these two approaches often helps resolving difficult cases, but it is not always feasible. The physiological variability analysis I offered here circumvents this problem by exploiting naturally occurring variabilities in electrophysiological properties of photoreceptors in the same species or breed. While it has several shortcomings, including nonequivalence of correlation and causation, and a need to obtain a large number of data points, its advantages are appealing.

Acknowledgments

The author thanks Dr. Jeremy Niven for many insightful discussions and Prof. Andrew S. French for help with the manuscript.

The author declares no competing financial interests.

Sharona E. Gordon served as editor.

Submitted: 6 November 2017
Revised: 11 May 2018
Accepted: 28 June 2018

References

Abou Tayoun, A.N., X. Li, B. Chu, R.C. Hardie, M. Juusola, and P.J. Dolph. 2011. The Drosophila SK channel (dSK) contributes to photoreceptor performance by mediating sensitivity control at the first visual network. *J. Neurosci.* 31:13897–13910. https://doi.org/10.1523/JNEUROSCI.3134-11.2011

Baden, T., T. Euler, M. Weckström, and L. Lagnado. 2013. Spikes and ribbon synapses in early vision. *Trends Neurosci.* 36:480–488. https://doi.org/10.1016/j.tins.2013.04.006

Cuttle, M.F., W. Hevers, S.B. Laughlin, and R.C. Hardie. 1995. Diurnal modulation of photoreceptor potassium conductance in the locust. *J. Comp. Physiol. A Neuroethol. Sens. Neural Behav. Physiol.* 176:307–316. https://doi.org/10.1007/BF00219056

Elkins, T., and B. Ganetzky. 1988. The roles of potassium currents in Drosophila flight muscles. *J. Neurosci.* 8:428–434. https://doi.org/10.1523/JNEUROSCI.08-02-00428.1988

Frolov, R.V. 2015. Biophysical properties of photoreceptors in Corixa punctata facilitate diurnal life-style. *Vision Res.* 111(Pt A):75–81. https://doi.org/10.1016/j.visres.2015.03.026

Frolov, R.V. 2016. Current advances in invertebrate vision: insights from patch-clamp studies of photoreceptors in apposition eyes. *J. Neurophysiol.* 116:709–723. https://doi.org/10.1152/jn.00288.2016

Frolov, R.V., and S. Singh. 2014. Celecoxib and ion channels: a story of unexpected discoveries. *Eur. J. Pharmacol.* 730:61–71. https://doi.org/10.1016/j.ejphar.2014.02.032

Frolov, R., and M. Weckström. 2014. Developmental changes in biophysical properties of photoreceptors in the common water strider (Gerris lacustris): better performance at higher cost. *J. Neurophysiol.* 112:913–922. https://doi.org/10.1152/jn.00239.2014

Frolov, R., E.V. Immonen, M. Vähäsöyrinki, and M. Weckström. 2012. Postembryonic developmental changes in photoreceptors of the stick insect Carausius morosus enhance the shift to an adult nocturnal life-style. *J. Neurosci.* 32:16821–16831. https://doi.org/10.1523/JNEUROSCI.2612-12.2012

Frolov, R.V., E.V. Immonen, and M. Weckström. 2014. Performance of blue- and green-sensitive photoreceptors of the cricket Gryllus bimaculatus. *J. Comp. Physiol. A Neuroethol. Sens. Neural Behav. Physiol.* 200:209–219. https://doi.org/10.1007/s00359-013-0879-6

Frolov, R., E.V. Immonen, and M. Weckström. 2016. Visual ecology and potassium conductances of insect photoreceptors. *J. Neurophysiol.* 115:2147–2157. https://doi.org/10.1152/jn.00795.2015

Frolov, R.V., A. Matsushita, and K. Arikawa. 2017. Not flying blind: a comparative study of photoreceptor function in flying and non-flying cockroaches. *J. Exp. Biol.* 220:2335–2344. https://doi.org/10.1242/jeb.159103

Gomez-Ospina, N., G. Panagiotakos, T. Portmann, S.P. Pasca, D. Rabah, A. Budzillo, J.P. Kinet, and R.E. Dolmetsch. 2013. A promoter in the coding region of the calcium channel gene CACNA1C generates the transcription factor CCAT. *PLoS One.* 8:e60526. https://doi.org/10.1371/journal.pone.0060526

Hardie, R.C., D. Voss, O. Pongs, and S.B. Laughlin. 1991. Novel potassium channels encoded by the Shaker locus in Drosophila photoreceptors. *Neuron.* 6:477–486. https://doi.org/10.1016/0896-6273(91)90255-X

Heras, F.J.H., M. Vähäsöyrinki, and J.E. Niven. 2018. Modulation of voltage-dependent K+ conductances in photoreceptors trades off investment in contrast gain for bandwidth. *bioRxiv*. https://doi.org/10.1101/344325 (Preprint posted June 12, 2018)

Hevers, W., and R.C. Hardie. 1995. Serotonin modulates the voltage dependence of delayed rectifier and Shaker potassium channels in Drosophila photoreceptors. *Neuron.* 14:845–856. https://doi.org/10.1016/0896-6273(95)90228-7

Immonen, E.V., A.S. French, P.H. Torkkeli, H. Liu, M. Vähäsöyrinki, and R.V. Frolov. 2017. EAG channels expressed in microvillar photoreceptors are unsuited to diurnal vision. *J. Physiol.* 595:5465–5479. https://doi.org/10.1113/JP273612

Juusola, M., R.O. Uusitalo, and M. Weckström. 1995. Transfer of graded potentials at the photoreceptor-interneuron synapse. *J. Gen. Physiol.* 105:117–148. https://doi.org/10.1085/jgp.105.1.117

Juusola, M., J.E. Niven, and A.S. French. 2003. Shaker K+ channels contribute early nonlinear amplification to the light response in Drosophila photoreceptors. *J. Neurophysiol.* 90:2014–2021. https://doi.org/10.1152/jn.00395.2003

Krause, Y., S. Krause, J. Huang, C.H. Liu, R.C. Hardie, and M. Weckström. 2008. Light-dependent modulation of Shab channels via phosphoinositide depletion in Drosophila photoreceptors. *Neuron.* 59:596–607. https://doi.org/10.1016/j.neuron.2008.07.009

Laughlin, S.B. 1996. Matched filtering by a photoreceptor membrane. *Vision Res.* 36:1529–1541. https://doi.org/10.1016/0042-6989(95)00242-1

Laughlin, S.B., and M. Weckström. 1993. Fast and slow photoreceptors — a comparative study of the functional diversity of coding and conductances in the Diptera. *J. Comp. Physiol. A Neuroethol. Sens. Neural Behav. Physiol.* 172:593–609. https://doi.org/10.1007/BF00213682

Linder, C.C. 2006. Genetic variables that influence phenotype. *ILAR J.* 47:132–140. https://doi.org/10.1093/ilar.47.2.132

Niven, J.E., M. Vähäsöyrinki, and M. Juusola. 2003a. Shaker K(+)-channels are predicted to reduce the metabolic cost of neural information in Drosophila photoreceptors. *Proc. Biol. Sci.* 270(Suppl 1):S58–S61. https://doi.org/10.1098/rsbl.2003.0010

Niven, J.E., M. Vähäsöyrinki, M. Kauranen, R.C. Hardie, M. Juusola, and M. Weckström. 2003b. The contribution of Shaker K+ channels to the information capacity of Drosophila photoreceptors. *Nature.* 421:630–634. https://doi.org/10.1038/nature01384

Niven, J.E., M. Vähäsöyrinki, M. Juusola, and A.S. French. 2004. Interactions between light-induced currents, voltage-gated currents, and input signal properties in Drosophila photoreceptors. *J. Neurophysiol.* 91:2696–2706. https://doi.org/10.1152/jn.01163.2003

Salmela, I., E.V. Immonen, R. Frolov, S. Krause, Y. Krause, M. Vähäsöyrinki, and M. Weckström. 2012. Cellular elements for seeing in the dark: voltage-dependent conductances in cockroach photoreceptors. *BMC Neurosci.* 13:93. https://doi.org/10.1186/1471-2202-13-93

Weckström, M., and S.B. Laughlin. 1995. Visual ecology and voltage-gated ion channels in insect photoreceptors. *Trends Neurosci.* 18:17–21. https://doi.org/10.1016/0166-2236(95)93945-T

Weckström, M., R.C. Hardie, and S.B. Laughlin. 1991. Voltage-activated potassium channels in blowfly photoreceptors and their role in light adaptation. *J. Physiol.* 440:635–657. https://doi.org/10.1113/jphysiol.1991.sp018729